Electron-impact excitation of some low-lying levels of neon

Luiz E. Machado*
Department of Chemistry, California Institute of Technology, Pasadena, California 91125

Emerson P. Leal
Departamento de Fisica, Universidade Federal de São Carlos, 13560 São Carlos, São Paulo, Brazil

George Csanak
Theoretical Division, Los Alamos National Laboratory, Los Alamos, New Mexico 87545†
and Instituto de Fisica, Universidade Estadual de Campinas, 13100 Campinas, São Paulo, Brazil.
(Received 15 February 1983)

First-order many-body theory has been used to calculate the differential and integral cross sections for electron-impact excitation of all the $3s,3s'$ levels, and certain of the $3p,3p'$ levels of neon, for incident electron energies ranging from 20 to 120 eV. The resulting differential cross sections for the excitation of the optically allowed $^1P_1$ and the $^3P_1$ levels show, for the $10° \leq \theta \leq 80°$ angular range, a discrepancy no greater than 15% when compared with recent experimental results, except for very few points. Spin-orbit coupling was included in the wave functions and its effect on determining the differential cross sections for the $^3P_1$ level was found to be very important for scattering angles less than 40°. For the differential cross sections of the other $3s,3s'$ levels the discrepancy in the $30° \leq \theta \leq 80°$ range is only slightly larger than the experimental errors. For the $3p,3p'$ levels considered here, we have found strong disagreement with experimental data and there is also substantial disagreement among the various theoretical results.

I. INTRODUCTION

The electron-impact excitation of neon is of considerable scientific interest both from the basic and from the applied physics point of view. From the applied physics point of view, neon is a component of several important laser systems (e.g., He-Ne, KrF, and XeCl) wherein electronic-impact processes are occuring.[1] From the basic physics point of view, neon is part of the rare-gas series (He, Ne, Ar, Kr, and Xe) where *LS* coupling changes into *jl* coupling and then to *jj* coupling in the spectroscopic description of the states of these atomic systems.[2] Electron-impact excitation of helium has been the subject of a large number of theoretical and experimental studies[3] and detailed measurements were recently reported for the differential cross section (DCS) for elastic and inelastic electron scattering from argon[4,5] and krypton.[4,6] These experiments were the first where *all* the $4s,4s'$ levels[7] of argon were resolved in a DCS experiment. They have now been complemented by obtaining elastic and inelastic electron scattering DCS's for neon where several (including *all* $3s,3s'$) *levels* were resolved in the electron energy-loss spectra.[8,9] The only previous inelastic DCS measurements on neon which resolved *some levels* were that of Tam and Brion[10] for the excitation of the $3p'[\frac{1}{2}]_0$ level[11] and Roy and Carette[12] who reported relative DCS's for several resolved levels. Prior to that the only *inelastic* DCS measurement was the one reported by Nicoll and Mohr[13] in 1933 for the unresolved $3s,3s'$ levels. On the other hand, there are several reports on the measurement of "apparent" (optical) integrated cross sections (ICS's) for the electron-impact excitation of neon. The principal reason is that an apparent ICS can be measured by various optical techniques, which, however, usually contain an unknown contribution from cascade effects. The first (relative) optical excitation functions for neon were reported by Hanle.[14] Subsequently Herrmann[15] reported measurements of maxima of absolute optical excitation functions and Zapesochnyi and Feltsan[16] measured optical excitation functions for several $3p,3p'$ levels. Sharpton *et al.*[17] reported optical excitation functions and ICS's for some fifty levels of neon (but not for the $3s,3s'$ levels). An ICS for the optically allowed $3s'[\frac{1}{2}]_1^o$ level was reported by de Jongh[18] and relative excitation functions for the same level by Van Raan.[19] Tan *et al.*[20] reported absolute excitation functions for the excitation of the $3s'[\frac{1}{2}]_1^o$ level but these results, like those of Van Raan,[19] were not corrected for cascade. Recently a laser-excitation-fluorescence technique was used by Phillips *et al.*[21] and Miers *et al.*[22] to measure ICS's for the excitation of the $3s[1\frac{1}{2}]_0^o$ and $3s[1\frac{1}{2}]_2^o$ metastable and the $3s[1\frac{1}{2}]_1^o$ and $3s'[\frac{1}{2}]_1^o$ optically allowed levels, respectively. Teubner *et al.*[23] reported the use of time-of-flight technique to measure the sum of the ICS's for the excitation of the two $3s$ metastable levels.

On the theoretical side, the majority of calculations reported for the electron-impact excitation of neon were of the Born or Born-Ochkur type, and mainly for the ICS. It is interesting to note though that the first reported calculation for the electron-impact excitation of the unresolved $3s,3s'$ levels of neon by Massey and Mohr[24] was with the distorted-wave approximation with the additional simplification that the asymptotic form of the distorted waves were used and the partial-wave phase shifts were calculated using Jeffrey's (also called WKB) approximation.

Their results were compared with the unresolved DCS results of Nicoll and Mohr[13] and showed qualitative agreement. Veldre *et al.*[25] calculated ICS's for a large number of levels of neon using the Born approximation. They used the hydrogenic functions for both the ground- and excited-state orbitals and considered *LS*, *jl*, and *jj* coupling schemes for the description of the excited states. Large number of transitions were considered including all $3s,3s'$ and $3p,3p'$ levels. Boikova and Fradkin[26] used the Born-Ochkur approximation to calculate ICS's for the excitation of the $3p,3p'$ levels and a detailed study was made for the various coupling cases and results for the ICS's reported. Sharpton *et al.*[17] reported Born and Born-Ochkur ICS results for the excitation of a large number of levels of neon, where the spin-orbit coupling effect was introduced into the wave functions of the excited states via a semiempirical procedure. Albat and Gruen[27] reported Born calculation results for the DCS and ICS of the excitation of the $3s'[\frac{1}{2}]_1^o$ level. In their work, a detailed study was made with respect to electron correlation effects in the ground- and excited-state wave functions and spin-orbit coupling in the excited state was included by a semiempirical method. Mileev *et al.*[28] used the multiple-collision diffraction theory[29] for the calculation of the ICS of the $3s'[\frac{1}{2}]_1^o$ level excitation in the *LS* coupling scheme. Recently, Theodosiou[30] reported ICS results for the excitation of the *LS* coupled $3s$ and $3p$ levels using the Vainshtein-Presnyakov-Sobel'man approximation (VPSA).[31]

There are few theoretical results available for inelastic DCS's for neon. Following the simplified DWA calculation of Massey and Mohr[24] (already mentioned), Ganas and Green[32] reported Born DCS's for the excitation of the $3s,3s'$ levels using *LS* coupled wave functions. Lins de Barros and Brandi[33] reported Born-Ochkur DCS results where the *jl* coupling scheme was used for the description of the excited states of neon. Sawada *et al.*[34] applied the distorted-wave approximation (DWA) for the study of the electron-impact excitation of the $3s,3s'$ unresolved levels of neon. In their work, a semiempirical distorting potential was used (with adjustable parameters), the target states were described within the *LS* coupling scheme, and two different distorting potentials were used in the direct and exchange amplitudes (which was justified by an heuristic argument). The results were compared with the experimental results of Nicoll and Mohr[13] for the unresolved $3s,3s'$ DCS's. Recently, Balashov *et al.*[35] completed a detailed study for the excitation of the unresolved $3s,3s'$ levels of neon. They used the DWA as well as various versions of the multichannel diffraction approximation (MCDA) of Feshbach and Hüfner.[36] The *LS* coupling scheme was used for the target states, thus spin-orbit coupling effects were completely ignored. The distortion potential in their DWA scheme was a sum of static, local-exchange, semiempirical polarization and absorption terms. DCS data were presented but not compared with experiment. They also presented ICS results which was compared with the experimental results of de Jongh[18] and van Raan.[19]

Practically all of the theoretical results summarized above for electron-impact excitation of neon were either Born-type (Born, Born-Ochkur) theories, with or without spin-orbit coupling effects in the target states, or distorted-wave theories using the *LS*-coupling scheme. Thus it appeared worthwhile to implement a theory which incorporates both spin-orbit coupling effects into the target states and considers the distortion effect of the target on the free electron. For this purpose the first-order many-body theory (FOMBT) was chosen. The FOMBT was formulated by Csanak *et al.*[37] and can be considered as one form of the distorted-wave approximation (DWA), as has been shown by Rescigno *et al.*[38] The relationship of the FOMBT to the more conventional forms of the DWA has also been discussed by Pindzola and Kelly,[39] Calhoun *et al.*,[40] Madison,[41] and Winters,[42] and a comprehensive review has been given about these, and related methods by Bransden and McDowell.[43] The derivation, physical principles, and applicability of the DWA has been discussed in the classic texts of Mott and Massey,[44] Bethe and Jackiw,[45] Massey *et al.*,[46] and Sobelman *et al.*[47] and in reviews by Moiseiwitsch and Smith,[48] and Brandsen and McDowell.[43]

The FOMBT scattering matrix contains direct and exchange terms, and the electron scattering orbitals are calculated in the static-exchange field of the ground-state target.

The FOMBT neglects (as does the DWA) "channel-coupling" effects between excited states, the "back-coupling" effect of an inelastic channel to the elastic channel and the effect of the final target state upon the scattered electron. These higher-order effects can be taken into consideration either by a second-order many-body theory (SOMBT), such as formulated by Csanak *et al.*,[49] or by the more conventional close-coupling approximation of Burke and Schey[50] or *R*-matrix theory of Burke *et al.*[51] The *R*-matrix approach has been recently applied by Fon *et al.*[52] to the calculation of the DCS for elastic electron scattering by argon but no inelastic DCS results have been reported thus far for neon or argon using the *R*-matrix method.

Thus, the aim of the present work is to report DCS and ICS results of a first-order many-body theory (FOMBT) calculation for the electron-impact excitation of all the $3s,3s'$ levels and some of the $3p,3p'$ levels of neon. The levels considered in this report will be the $3s[1\frac{1}{2}]_1^o$, $3s[1\frac{1}{2}]_2^o$, $3s'[\frac{1}{2}]_0^o$, $3s'[\frac{1}{2}]_1^o$ levels as well as the $3p[\frac{1}{2}]_0$ and $3p'[\frac{1}{2}]_0$ levels. The FOMBT has been previously applied for the calculation of the excitation of several levels of helium[53,54] and argon.[55] The present calculation follows closely the work of Padial *et al.*[55] on argon. The results of the FOMBT for the coherence and correlation parameters for the optically allowed $3s[1\frac{1}{2}]_1^o$ and $3s'[\frac{1}{2}]_1^o$ levels of neon have been already reported.[56] The DCS and ICS results will be compared with the recent experimental results of Register *et al.*,[9] and for the ICS of the excitation for the $3p[\frac{1}{2}]_0$ level will be compared with the experimental data of Sharpton *et al.*[17]

II. THEORETICAL FOUNDATION

The FOMBT for electron atom inelastic scattering was introduced by Csanak *et al.*[37] The detailed description of the theory and its application to atoms where spin-orbit

coupling effect is taken into consideration in the target states was given by Padial *et al.*[55]

A. Brief review of the FOMBT

The FOMBT belongs to the class of distorted-wave approximations (DWA). The S matrix is given in the FOMBT by the formula,

$$S^{\mathrm{FOMBT}}_{0\tilde{p},n\tilde{q}} = -2\pi i\delta(\epsilon_{\tilde{p}}-\epsilon_{\tilde{q}}-\omega_n)T^{\mathrm{FOMBT}}_{0\tilde{p},n\tilde{q}}$$
$$= 2\pi i\delta(\epsilon_{\tilde{p}}-\epsilon_{\tilde{q}}-\omega_n)\int dx_1 dx_2 f^{(-)\mathrm{HF}^*}_{\tilde{q}}(x_1) \times f^{(+)\mathrm{HF}}_{\tilde{p}}(x_2)V^{\mathrm{RPA}}_{0n}(x_1,x_2)\ , \tag{1}$$

where $x_1(x_2)$ refers to both the spatial $\vec{r}_1(\vec{r}_2)$ and spin $\sigma_1(\sigma_2)$ coordinates, $\tilde{p}(\tilde{q})$ refers to both the momentum $\vec{p}(\vec{q})$ and spin $m_{s_1}(m_{s_2})$ of the incident (scattered) electron, and ω_n to the excitation energy of the state n. $V^{\mathrm{RPA}}_{0n}(x_1,x_2)$ is defined by the formula

$$V^{\mathrm{RPA}}_{0n}(x_1,x_2)=\delta(x_1-x_2)\int \frac{dx'}{|\vec{r}_1-\vec{r}'|}X^{\mathrm{RPA}}_n(x',x') - \frac{1}{|\vec{r}_1-\vec{r}_2|}X^{\mathrm{RPA}}_n(x_2,x_1)\ , \tag{2}$$

where $X^{\mathrm{RPA}}_n(x_2,x_1)$ is the transition density matrix between states n and 0 (the ground state) calculated in the random-phase approximation (RPA),[57] and

$$\delta(x_1-x_2)=\delta(\vec{r}_1-\vec{r}_2)\delta_{\sigma_1\sigma_2}\ ,$$

where $\delta(\vec{r})$ is the Dirac delta function and $\delta_{\sigma_1\sigma_2}$ is the Kronecker delta symbol. The transition density matrix is defined by the formula

$$X^{\mathrm{RPA}}_n(x,x')=\langle\Psi_n\,|\,\psi^\dagger(x)\psi(x')\,|\,\Psi_0\rangle\ , \tag{3}$$

where $|\Psi_0\rangle$ and $|\Psi_n\rangle$ refer to the state vectors of the ground (0) and excited (n) states of the target, respectively, and $\psi(x)$ is the electron field operator in the Schrödinger representation. The transition density matrix can be expressed in terms of the wave functions of the ground $[\Psi_0(x_1x_2,\ldots,x_n)]$ and excited $[\Psi_n(x_1x_2,\ldots,x_n)]$ states, respectively, in the form

$$X^{\mathrm{RPA}}_n(x,x')=N\int \Psi^*_n(x,x_2,\ldots,x_N)\Psi_0(x',x_2,\ldots,x_N) \times dx_2\cdots dx_N\ , \tag{4}$$

where N refers to the number of electrons in the system. In Eq. (1), $f^{(+)\mathrm{HF}}_{\tilde{p}}(x)$ and $f^{(-)\mathrm{HF}}_{\tilde{q}}(x)$ are the electron scattering orbitals in the Hartree-Fock (HF) (also called static-exchange) approximation with outgoing wave and incoming wave boundary conditions, respectively.

Inspection of the S-matrix formula given in Eq. (1), along with the expressions for V^{RPA}_{0n} and X^{RPA}_n given by Eqs. (2) and (3), shows clearly that the FOMBT incorporates first-order direct and exchange excitation effects and includes distortion of the free-electron wave function. As mentioned above, coupling between excited state channels, the back-coupling effect upon the elastic channel and the effect of the final target state upon the scattered electron are neglected. These latter effects are of second order and they can be incorporated within the SOMBT,[54] close-coupling,[50] or R-matrix theories.[51]

B. Analytical and numerical details

The following simplifications were introduced in calculating $T^{\mathrm{FOMBT}}_{0\tilde{p},n\tilde{q}}$ which was defined by Eq. (1):

(i) Spin-orbit coupling effects were neglected in the calculation of the $f^{(+)\mathrm{HF}}_{\tilde{p}}(x)$ and $f^{(-)\mathrm{HF}}_{\tilde{q}}(x)$ orbitals. Since spin-polarization effects are small for neon[58] this approximation appears to be well justified. As a consequence, the orbitals can be factored in the form

$$f^{(+)\mathrm{HF}}_{\tilde{p}}(x)=f^{(+)\mathrm{HF}}_{\vec{p}}(\vec{r})\eta_{m_{s_1}}(\sigma)\ , \tag{5a}$$

$$f^{(-)\mathrm{HF}}_{\tilde{q}}(x)=f^{(-)\mathrm{HF}}_{\vec{q}}(\vec{r})\eta_{m_{s_2}}(\sigma)\ , \tag{5b}$$

where $\eta_{m_s}(\sigma)$ is the Pauli spin-function.

(ii) In calculating the transition density matrix instead of solving the RPA equations (as would be required by the FOMBT) the following procedure was used. The ground- and excited-state wave functions were constructed separately and the transition-density was calculated subsequently using these functions. [See Eq. (4).] The LS coupled HF wave function was used for the ground state since the spin-orbit interaction energy is zero for a closed-shell state. The excited state wave functions were constructed as linear combinations of LS-coupled fixed-core Hartree-Fock (FCHF) wave functions.[59] The procedure for the $3s,3s'$ states of neon is identical to the one used by Padial *et al.*[55] for the $4s,4s'$ states of argon and is based on the method of Cowan and Andrew[60] and Cowan.[61] In the present case we can write, using the notation of Padial *et al.*,[55]

$$|\,3s'[\tfrac{1}{2}]^e_1;M_J\rangle = b\,|\,[(2p)^5 3s]3^1P_1;M_J\rangle + a\,|\,[(2p)^5 3s]3^3P_1;M_J\rangle\ , \tag{6a}$$

$$|\,3s[1\tfrac{1}{2}]^o_1;M_J\rangle = -a\,|\,[(2p)^5 3s]3^1P_1;M_J\rangle + b\,|\,[(2p)^5 3s]3^3P_1;M_J\rangle\ . \tag{6b}$$

For neon, the value of the a and b parameters were provided by Cowan[61] as

$$a=0.266,\quad b=0.964\ . \tag{6c}$$

The wave functions for the $3p'[\frac{1}{2}]_0$ and $3p[\frac{1}{2}]_0$ states were constructed analogously using the form

$$|\,3p'[\tfrac{1}{2}]_0;M_J=0\rangle = \bar{a}\,|\,[(2p)^5 3p]3^1S_0;M_J=0\rangle + \bar{b}\,|\,[(2p)^5 3p]3^3P_0;M_J=0\rangle\ , \tag{7a}$$

$$|3p[\tfrac{1}{2}]_0;M_J=0\rangle-\bar{b}\,|[(2p)^5 3p]3^1S_0;M_J=0\rangle$$
$$+\bar{a}\,|[(2p)^5 3p]3^3P_0;M_J=0\rangle\ , \tag{7b}$$

where[62]

$$\bar{a}=0.99,\quad \bar{b}=0.14\ . \tag{7c}$$

In the present calculation the $3s$ orbitals that enter the LS coupled wave functions of the $[(2p)^5 3s]3^1P_1$ and $[(2p)^5 3s]3^3P_1$ states, respectively, were calculated from the appropriate and different FCHF equations[63] as opposed to Padial *et al.* who used the FCHF equations for the $[(3p)^5 4s]4^1P_1$ states in *obtaining* the $4s$ orbitals for both the 4^1P_1 and 4^3P_1 states. Analogously, the $3p$ orbitals of the $[(2p)^5 3p]3^1S_0$ and $[(2p)^5 3p]3^3P_0$ states were obtained from the appropriate FCHF equations. In the calculation of the $3p$ orbitals, they were orthogonalized to the core $2p$ orbitals.

The transition density matrix between the LS coupled 3^1S_0 ground state and the $[(2p)^5 3s]3^1P_1$ and $[(2p)^5 3s]3^3P_1$ excited states can be calculated in close analogy to the case of argon detailed by Padial *et al.*[55] The relevant equations are identical to that of argon if the $3p\rightarrow 2p, 4s\rightarrow 3s$ substitutions are made and they will not be given here.

For the case of the calculation of the transition density matrix between the $^1S_0$ ground state on the one hand and the $[(2p)^5 3p]3^1S_0$ or $[(2p)^5 3p]3^3P_0$ LS-coupled excited states on the other hand, one obtains the following formulas (using the notation of Padial *et al.*[55] again):

$$X_{0,3p^{2S+1}L;M_L M_s}(x_1,x_2)$$
$$=X_{0,3p^{2S+1}L,M_L}(\vec{r}_1,\vec{r}_2)\xi_{S,M_s}(\sigma_1,\sigma_2)\ , \tag{8}$$

where

$$X_{0,3p^{2S+1}L;M_L}(\vec{r}_1,\vec{r}_2)=R_{2p}(r_2)R^{(S)}_{3p}(r_1)\sum_{m_\alpha m_i}(-1)^{m_\alpha}(1-m_\alpha 1m_i\,|\,11LM_L)Y_{1m_\alpha}(\hat{r}_2)Y_{1m_i}(\hat{r}_1)\ . \tag{9}$$

Here $R^{(S)}_n(r)$ is the radial part of the excited orbital. The spin-functions $\xi_{S,M_s}(\sigma_1,\sigma_2)$ are given by Padial *et al.*[55]

The calculational procedure of the T matrix and DCS of the $3s$ and $3s'$ levels is identical to the one used by Padial *et al.*[55] for the $4s$ and $4s'$ levels of argon and can be easily adopted to the present case if in all formulas of Padial *et al.*[55] the $4\rightarrow 3, 4s\rightarrow 3s, 4s'\rightarrow 3s', 3p\rightarrow 2p, 3s\rightarrow 2s$ substitutions are made.

For the excitation of the $3p'[j]_0, 3p[j]_0$ levels the following formulas hold:

$$\left[\frac{d\sigma}{d\Omega}\right]_{3p'[\frac{1}{2}]_0}=\frac{1}{4\pi^2}\frac{q}{p}\left[\frac{\bar{a}^2}{2}\,|\,2T^0_{L=0,M_L=0,S=0}-T^E_{L=0,M_L=0,S=0}\,|^2\right.$$
$$\left.+\frac{\bar{b}^2}{6}(\,|\,T^E_{L=1,M_L=1,S=1}\,|^2+\,|\,T^E_{L=1,M_L=0,S=1}\,|^2+\,|\,T^E_{L=1,M_L=-1,S=1}\,|^2)\right] \tag{10a}$$

and

$$\left[\frac{d\sigma}{d\Omega}\right]_{3p[\frac{1}{2}]_0}=\frac{1}{4\pi^2}\frac{q}{p}\left[\frac{\bar{b}^2}{2}\,|\,2T^D_{L=0,M_L=0,S=0}-T^E_{L=0,M_L=0,S=0}\,|^2\right.$$
$$\left.+\frac{\bar{a}^2}{6}(\,|\,T^E_{L=1,M_L=1,S=1}\,|^2+\,|\,T^E_{L=1,M_L=0,S=L}\,|^2+\,|\,T^E_{L=1,M_L=-1,S=1}\,|^2)\right]\ , \tag{10b}$$

where $T^D_{L,M,S}$ and $T^E_{L,M,S}$ are defined by the equations

$$T^D_{L,M_L,S}=\int\int d\vec{r}_1 d\vec{r}_2 f^{(+)\mathrm{HF}}_{\vec{p}}(\vec{r}_1)f^{(-)\mathrm{HF}*}_{\vec{q}}(\vec{r}_1)V(\vec{r}_1-\vec{r}_2)$$
$$\times X_{2p,3p^{2S+1}L,M_L}(\vec{r}_2,\vec{r}_2)\ , \tag{11a}$$

$$T^E_{L,M_L,S}=\int\int d\vec{r}_1 d\vec{r}_2 f^{(+)\mathrm{HF}}_{\vec{p}}(\vec{r}_1)f^{(-)\mathrm{HF}*}_{\vec{q}}(\vec{r}_2)V(\vec{r}_1-\vec{r}_2)$$
$$\times X_{2p,3p^{2S+1}L,M_L}(\vec{r}_2,\vec{r}_1)\ , \tag{11b}$$

where

$$V(\vec{r}_1-\vec{r}_2)=1/|\,\vec{r}_1-\vec{r}_2\,|$$

is the Coulomb interaction potential. The numerical technique adopted for the calculation of $T^D_{L,M,S}$ and $T^E_{L,M,S}$ is identical to that used by Padial *et al.*[55] The $f^{(+)\mathrm{HF}}_{\vec{p}}(\vec{r})$ and $f^{(-)\mathrm{HF}}_{\vec{q}}(\vec{r})$ orbitals were expanded in terms of partial waves and the radial parts calculated by numerically integrating the static exchange equations using the computer program of Bates.[59] In calculating the $T^D_{L,M,S}$ matrix the technique of adding and subtracting the Born T matrix was used.[50] In calculating the radial integrals, again numerical integration was used for an interval $[0,R_0]$ and approximate analytical forms were used for the $[R_0,\infty]$ interval.[55] The value of R_0 for neon was typically $R_0=80.0$ a.u.

III. RESULTS AND DISCUSSIONS

In this section the DCS's and ICS's obtained from application of the FOMBT calculation described in the previous section will be reported for excitation of the $3s[1\frac{1}{2}]^o_1, 3s[1\frac{1}{2}]^o_2, 3s'[\frac{1}{2}]^o_0, 3s'[\frac{1}{2}]^o_1$, and $3p[\frac{1}{2}]_0, 3p'[\frac{1}{2}]_0$ levels in neon and will be compared with available experimental data.

A. Differential cross sections (DCS's)

The first level to be discussed is $3s[1\frac{1}{2}]^o_1(^3P_1)$ because the importance of spin-orbit coupling in the final target state in determining the DCS is of primary interest in this study. As can be seen from Eqs. (6a) and (6c) this state is principally an LS coupled $^3P_1$ state with a contribution of less than 10% ($a^2 \approx 0.07$) originating from the LS coupled $^1P_1$ component. On the other hand, a small $^1P_1$ component mixed in with the $^3P_1$ state will strongly influence the DCS since it provides a mechanism for "direct" scattering which is usually more than an order of magnitude larger, at least for small angles, than the contribution from exchange scattering. This characteristic is supported by the present results shown on Fig. 1 in which the DCS results for the excitation of the $3s[1\frac{1}{2}]^o_1$ level are presented in both the "spin-orbit coupled" approximation (i.e., using the scheme as described in the previous section) and the LS-coupled approximation [i.e., using $a=1$ and $b=0$ in Eq. (6a)], for $E=30$- and 50-eV incident energies and compared with the recent experimental results of Register *et al.*[9] From Fig. 1 it is quite clear that in the $0 \leq \theta \leq 30°$ angular range the seemingly small $^1P_1$ component in the spin-orbit coupled wave function has a drastic effect on the forward scattering part of the DCS (and a corresponding effect on the ICS). From Fig. 1 it can also be seen that for $\theta > 50°$ angles the LS coupled and spin-orbit coupled results are practically identical signifying that for these angles the exchange scattering dominates. It can also be seen that at $E_0 = 30$-eV energy FOMBT badly fails for $\theta \geq 90°$ angles implying that the effects (channel-coupling, back-coupling, final-state interaction) not included in the FOMBT are important for the calculation of the DCS for these angles at 30 eV. It can be safely conjectured that higher-order exchange effects and influence of the potential of the final (excited) state of the target are important under these conditions. The FOMBT results are given in the spin-orbit coupled approximation for a series of energies in Table I.

The next level to be considered is the $3s'[\frac{1}{2}]^o_1(^1P_1)$ optically allowed, principally LS-coupled, $^1P_1$ level. Figure 2 shows the present spin-orbit coupled FOMBT results along with the experimental results of Register *et al.*[9] for the excitation of this level for incident energies of $E=30$, 50, and 100 eV. As can be seen from Fig. 2 for 100 eV, the theory agrees with the experiment (within experimental error) at practically every point. Figure 2 also shows that FOMBT deteriorates for $\theta > 80°$ angles as the energy decreases. This is probably due to the missing higher-order exchange terms as well as the effect of the final state on the scattered electron. Numerical results for the excitation of the $3s'[\frac{1}{2}]^o_1$ level are also given in Table I.

The DCS results for the excitation of the $3s'[\frac{1}{2}]^o_0(^3P_0)$ and $3s[1\frac{1}{2}]^o_2(^3P_2)$ metastable levels are given in Figs. 3

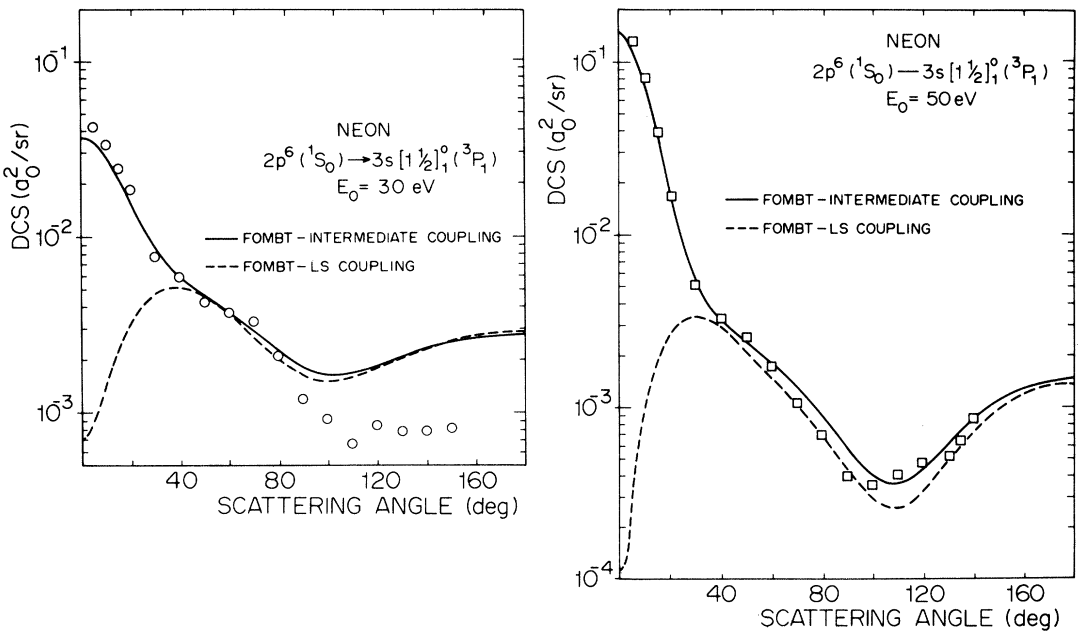

FIG. 1. Differential cross sections (DCS) for the excitation of $3s[1\frac{1}{2}]^o_1(^3P_1)$ level of neon, with (solid curve) and without (dashed curve) the inclusion of spin-orbit coupling. The circles (○) and squares (□) are the experimental points of Register *et al.* (Ref. 9) at incident electron energies of 30 and 50 eV, respectively. [Intermediate coupling: refers to final-state wave function given by Eqs. (6b) and (6c).]

TABLE I. Differential cross sections (in a_0^2/sr) for electron-impact excitation of the $3s'[\frac{1}{2}]_1^o$ and $3s[1\frac{1}{2}]_1^o$ levels of neon using intermediate coupling and the FOMBT.

Incident energy (eV) / Final level / Angle (deg)	20.0		30.0		40.0	
	$3s'[\frac{1}{2}]_1^o$	$3s[1\frac{1}{2}]_1^o$	$3s'[\frac{1}{2}]_1^o$	$3s[1\frac{1}{2}]_1^o$	$3s'[\frac{1}{2}]_1^0$	$3s[1\frac{1}{2}]_1^0$
0	0.325(−1)[a]	0.645(−2)	0.450(+0)	0.367(−1)	0.134(+1)	0.134(+1)
10	0.294(−1)	0.623(−2)	0.335(+0)	0.284(−1)	0.778(+0)	0.778(+0)
20	0.221(−1)	0.569(−2)	0.155(+0)	0.157(−1)	0.219(+0)	0.219(+0)
30	0.140(−1)	0.508(−2)	0.525(−1)	0.870(−2)	0.360(−1)	0.360(−1)
40	0.785(−2)	0.454(−2)	0.140(−1)	0.598(−2)	0.459(−2)	0.459(−2)
50	0.424(−2)	0.405(−2)	0.562(−2)	0.472(−2)	0.793(−2)	0.793(−2)
60	0.256(−2)	0.359(−2)	0.484(−2)	0.376(−2)	0.116(−1)	0.116(−1)
70	0.198(−2)	0.314(−2)	0.540(−2)	0.291(−2)	0.108(−1)	0.108(−1)
80	0.186(−2)	0.273(−2)	0.535(−2)	0.225(−2)	0.744(−2)	0.744(−2)
90	0.186(−2)	0.238(−2)	0.464(−2)	0.184(−2)	0.368(−2)	0.368(−2)
100	0.187(−2)	0.210(−2)	0.375(−2)	0.168(−2)	0.121(−2)	0.121(−2)
110	0.189(−2)	0.188(−2)	0.311(−2)	0.172(−2)	0.908(−3)	0.908(−3)
120	0.194(−2)	0.171(−2)	0.278(−2)	0.188(−2)	0.250(−2)	0.250(−2)
130	0.202(−2)	0.156(−2)	0.259(−2)	0.211(−2)	0.495(−2)	0.495(−2)
140	0.215(−2)	0.144(−2)	0.236(−2)	0.233(−2)	0.727(−2)	0.727(−2)
150	0.229(−2)	0.133(−2)	0.208(−2)	0.253(−2)	0.874(−2)	0.874(−2)
160	0.243(−2)	0.124(−2)	0.186(−2)	0.268(−2)	0.904(−2)	0.904(−2)
170	0.252(−2)	0.118(−2)	0.174(−2)	0.277(−2)	0.857(−2)	0.857(−2)
180	0.256(−2)	0.115(−2)	0.171(−2)	0.279(−2)	0.825(−2)	0.825(−2)

[a]The notation 0.325(−1) means 0.325×10^{-1}.

and 4, respectively, for $E=30$- and 50-eV impact energies, where the FOMBT results are compared with the recent experimental results of Register *et al.*[9] In the FOMBT no spin-orbit coupling effect is present in these target states so that the results presented are the same for both the spin-orbit coupled and LS-coupled cases. These levels are genuinely metastable. The difficulties in treating the excitation of metastable levels have been discussed (among others) by Bransden and McDowell[3] in conjunction with the excitation of the $n^3S,n^3P(n=2,3)$ levels of He. They

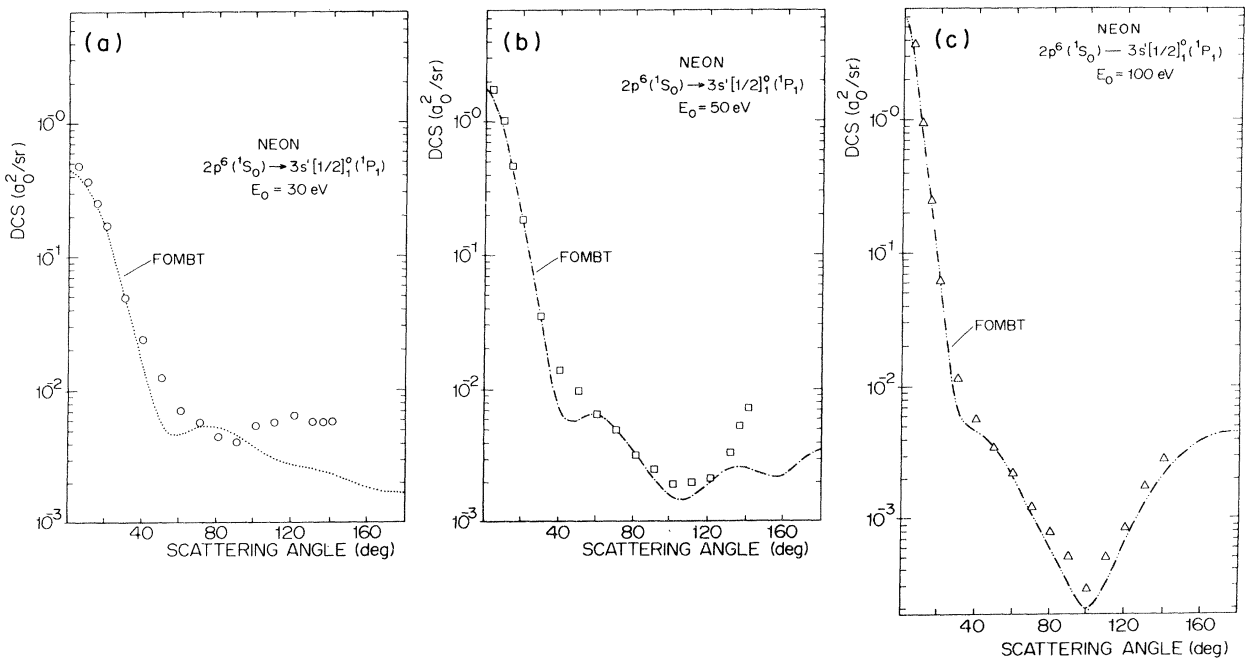

FIG. 2. DCS for the excitation of the $3s'[\frac{1}{2}]_1^o(^1P_1)$ level of neon, with the inclusion of the spin-orbit coupling. In all graphs the curves are the FOMBT results and circles (○), squares (□), and triangles (△) are the experimental points of Ref. 9. The incident electron energies are (a) 30 eV, (b) 50 eV, and (c) 100 eV. [Final-state wave function is given by Eqs. (6a) and (6c).]

TABLE I. (*Continued.*)

50.0		80.0		90.0		100.0	
$3s'[\frac{1}{2}]_1^o$	$3s[1\frac{1}{2}]_1^o$	$3s'[\frac{1}{2}]_1^o$	$3s[1\frac{1}{2}]_1^o$	$3s'[\frac{1}{2}]_1^o$	$3s[1\frac{1}{2}]_1^o$	$3s'[\frac{1}{2}]_1^o$	$3s[1\frac{1}{2}]_1^o$
0.186(+1)	0.149(+0)	0.438(+1)	0.342(+0)	0.613(+1)	0.480(+0)	0.790(+1)	0.618(+0)
0.859(+0)	0.689(−1)	0.954(+0)	0.737(−1)	0.843(+0)	0.653(−1)	0.722(+0)	0.557(−1)
0.192(+0)	0.175(−1)	0.103(+0)	0.900(−2)	0.634(−1)	0.554(−2)	0.396(−1)	0.346(−2)
0.324(−1)	0.560(−2)	0.933(−2)	0.172(−2)	0.658(−2)	0.909(−3)	0.529(−2)	0.587(−3)
0.711(−2)	0.323(−2)	0.456(−2)	0.957(−3)	0.465(−2)	0.544(−3)	0.404(−2)	0.384(−3)
0.624(−2)	0.241(−2)	0.410(−2)	0.712(−3)	0.339(−2)	0.397(−3)	0.247(−2)	0.258(−3)
0.660(−2)	0.182(−2)	0.286(−2)	0.527(−3)	0.206(−2)	0.278(−3)	0.135(−2)	0.169(−3)
0.523(−2)	0.132(−2)	0.176(−2)	0.375(−3)	0.107(−2)	0.185(−3)	0.666(−3)	0.105(−3)
0.335(−2)	0.892(−3)	0.995(−3)	0.262(−3)	0.577(−3)	0.139(−3)	0.404(−3)	0.850(−4)
0.208(−2)	0.578(−3)	0.530(−3)	0.190(−3)	0.305(−3)	0.113(−3)	0.243(−3)	0.755(−4)
0.153(−2)	0.402(−3)	0.337(−3)	0.145(−3)	0.202(−3)	0.970(−4)	0.210(−3)	0.694(−4)
0.155(−2)	0.362(−3)	0.433(−3)	0.130(−3)	0.325(−3)	0.952(−4)	0.334(−3)	0.723(−4)
0.203(−2)	0.441(−3)	0.847(−3)	0.151(−3)	0.715(−3)	0.110(−3)	0.623(−3)	0.834(−4)
0.252(−2)	0.617(−3)	0.157(−2)	0.206(−3)	0.140(−2)	0.148(−3)	0.116(−2)	0.113(−3)
0.241(−2)	0.848(−3)	0.254(−2)	0.293(−3)	0.222(−2)	0.202(−3)	0.176(−2)	0.152(−3)
0.219(−2)	0.108(−2)	0.358(−2)	0.397(−3)	0.315(−2)	0.272(−3)	0.248(−2)	0.207(−3)
0.234(−2)	0.128(−2)	0.449(−2)	0.491(−3)	0.408(−2)	0.352(−3)	0.324(−2)	0.273(−3)
0.311(−2)	0.140(−2)	0.512(−2)	0.557(−3)	0.452(−2)	0.394(−3)	0.355(−2)	0.304(−3)
0.358(−2)	0.145(−2)	0.534(−2)	0.581(−3)	0.456(−2)	0.399(−3)	0.353(−2)	0.304(−3)

wrote "the theoretical models assume that spin-orbit coupling is negligible (which is entirely justifiable for He), thus the direct matrix element vanishes, and the transition can proceed only by electron exchange. The exchange term is notoriously difficult to treat accurately, and higher-order corrections are probably required." These difficulties are also exemplified by the comparison of the experimental data with Ochkur-Rudge theoretical results for the excitation of the $A^3\Sigma_u$, $W^3\Delta_u$, $E^3\Sigma_g^+$, and $C^3\Pi_u$ levels by N_2 by Cartwright *et al.*[64] and for the excitation of the 2^3S and 2^3P levels of He, discussed by Thomas *et al.*[53] In light of these comments, the reasonably good agreement between the FOMBT results and the experimental data of Register *et al.*[9] for both the shape and the magnitude of the DCS for these two transitions in the $30° \leq \theta \leq 90°$ angular range is somewhat surprising. Whether this agreement is fortuitous or not awaits further experimental data and theoretical studies. The FOMBT results for excitation of these metastable levels are also presented in Table II for a variety of energies.

In the work reported here DCS results were also obtained for the excitation of the $3p[\frac{1}{2}]_0$ and $3p'[\frac{1}{2}]_0$ levels. It can be seen from Table I of Register *et al.*[9] that the $3p'[\frac{1}{2}]_0^o$ level has been resolved in their experiment. (In fact this level is one of the strongest transition and it was resolved by Tam and Brion[10] and Roy and Carette[12] also.)

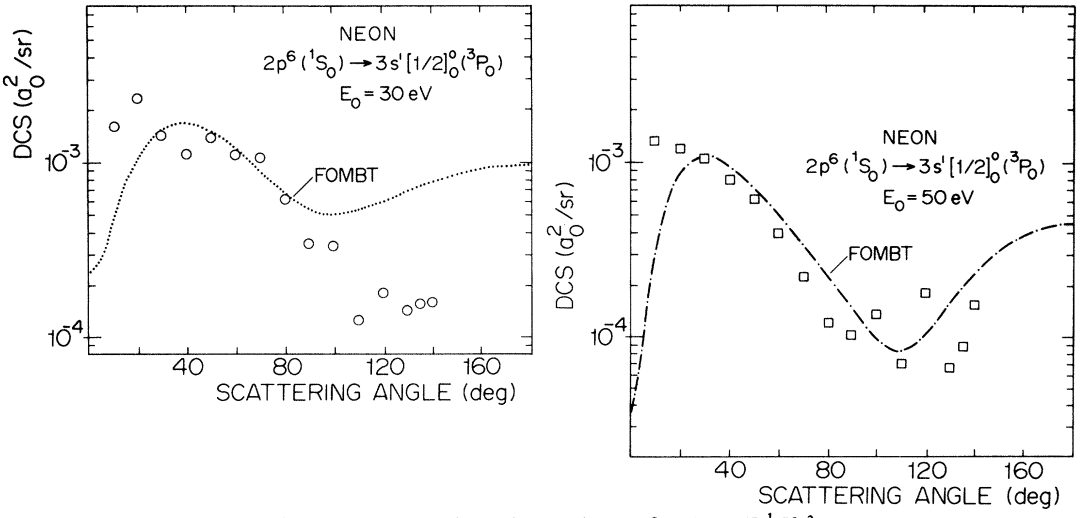

FIG. 3. Same as for Fig. 2, except here the results are for the $3s'[\frac{1}{2}]_0^o(^3P_0)$ level of neon.

TABLE II. Differential cross sections (in a_0^2/sr) for electron-impact excitation of the $3s'[\frac{1}{2}]_0^o(^3P_0)$ and $3s[1\frac{1}{2}]_2^o(^3P_2)$ levels of neon using the FOMBT.

Incident energy (eV) / Final level / Angle (deg)	20.0		30.0		40.0	
	$3s'[\frac{1}{2}]_1^o$	$3s[1\frac{1}{2}]_1^o$	$3s'[\frac{1}{2}]_1^o$	$3s[1\frac{1}{2}]_1^o$	$3s'[\frac{1}{2}]_1^0$	$3s[1\frac{1}{2}]_1^0$
0	0.125(−2)[a]	0.625(−2)	0.234(−3)	0.117(−2)	0.437(−4)	0.218(−3)
10	0.128(−2)	0.638(−2)	0.489(−3)	0.245(−2)	0.371(−3)	0.185(−2)
20	0.133(−2)	0.667(−2)	0.106(−2)	0.530(−2)	0.103(−2)	0.513(−2)
30	0.139(−2)	0.694(−2)	0.155(−2)	0.775(−2)	0.144(−2)	0.723(−2)
40	0.139(−2)	0.697(−2)	0.170(−2)	0.851(−2)	0.142(−2)	0.712(−2)
50	0.134(−2)	0.668(−2)	0.153(−2)	0.766(−2)	0.114(−2)	0.570(−2)
60	0.122(−2)	0.610(−2)	0.121(−2)	0.607(−2)	0.819(−3)	0.409(−2)
70	0.108(−2)	0.538(−2)	0.903(−3)	0.451(−2)	0.559(−3)	0.280(−2)
80	0.929(−3)	0.465(−2)	0.676(−3)	0.338(−2)	0.375(−3)	0.187(−2)
90	0.802(−3)	0.401(−2)	0.549(−3)	0.274(−2)	0.260(−3)	0.130(−2)
100	0.701(−3)	0.350(−2)	0.509(−3)	0.254(−2)	0.207(−3)	0.104(−2)
110	0.622(−3)	0.311(−2)	0.535(−3)	0.267(−2)	0.209(−3)	0.105(−2)
120	0.559(−3)	0.280(−2)	0.600(−3)	0.300(−2)	0.258(−3)	0.129(−2)
130	0.505(−3)	0.253(−2)	0.684(−3)	0.342(−2)	0.345(−3)	0.172(−2)
140	0.456(−3)	0.228(−2)	0.771(−3)	0.386(−2)	0.454(−3)	0.227(−2)
150	0.412(−3)	0.206(−2)	0.851(−3)	0.426(−2)	0.566(−3)	0.283(−2)
160	0.375(−3)	0.187(−2)	0.914(−3)	0.457(−2)	0.662(−3)	0.331(−2)
170	0.350(−3)	0.175(−2)	0.954(−3)	0.477(−2)	0.727(−3)	0.364(−2)
180	0.341(−3)	0.171(−2)	0.967(−3)	0.484(−2)	0.750(−3)	0.375(−2)

[a]The notation 0.125(−2) means 0.125×10^{-2}.

On the other hand, the $3p[\frac{1}{2}]_0$ level was unresolvable in their experiment (Feature 9) and the results of the present calculations cannot be directly compared with their experimental data or any other available experimental data. Figure 5 compares the recent experimental results for the excitation of the $3p'[\frac{1}{2}]_0$ level with the FOMBT results of the present calculation for $E=50$- and 100-eV impact energies. This figure shows poorer agreement between theory and experiment than for the $3s,3s'$ levels. This may be attributed to the following facts: (i) There are large numbers (a total of 10) of $3p,3p'$ levels close to each other and they may be strongly coupled, which is neglected in the FOMBT; (ii) there may be important correlation effects in the states belonging to these levels which are not included into the FCHF wave functions used in the present calculation; (iii) these levels have higher energies than the $3s,3s'$ levels and the coupling to these latter levels might play an important role, which is not considered in the FOMBT. The DCS results for the excitation of the $3p[\frac{1}{2}]_0$ and $3p'[\frac{1}{2}]_0$ levels are also given in Table III.

B. Integral cross sections

The ICS results of the present FOMBT calculation are compared in a series of figures by Register *et al.*[9] with

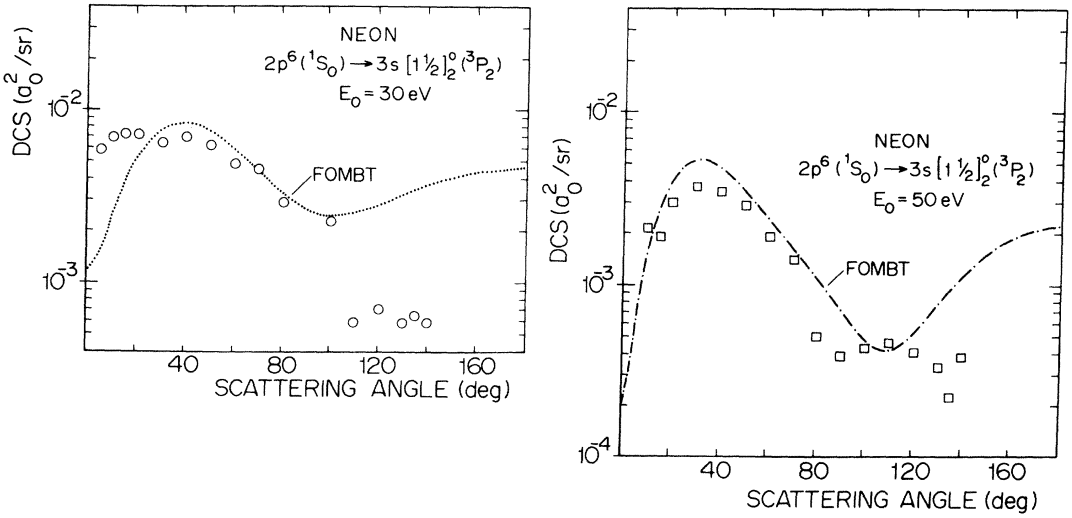

FIG. 4. Same as for Fig. 2, except here the results are for the $3s[1\frac{1}{2}]_2^o(^3P_2)$ level of neon.

TABLE II. (*Continued.*)

50.0		80.00		100.0		120.0	
$3s'[\frac{1}{2}]_0^e$	$3s[1\frac{1}{2}]_2^e$	$3s'[\frac{1}{2}]_0^e$	$3s[1\frac{1}{2}]_2^e$	$3s'[\frac{1}{2}]_0^e$	$3s[1\frac{1}{2}]_2^e$	$3s'[\frac{1}{2}]_0^e$	$3s[1\frac{1}{2}]_2^e$
0.371(−4)	0.185(−3)	0.578(−4)	0.289(−3)	0.541(−4)	0.270(−3)	0.479(−4)	0.240(−3)
0.335(−3)	0.166(−2)	0.232(−3)	0.116(−2)	0.176(−3)	0.881(−3)	0.135(−3)	0.673(−3)
0.873(−3)	0.437(−2)	0.415(−3)	0.208(−2)	0.250(−3)	0.125(−2)	0.158(−3)	0.788(−3)
0.111(−2)	0.554(−2)	0.337(−3)	0.169(−2)	0.146(−3)	0.732(−3)	0.666(−4)	0.333(−3)
0.966(−3)	0.483(−2)	0.198(−3)	0.988(−3)	0.686(−4)	0.343(−3)	0.277(−4)	0.138(−3)
0.702(−3)	0.351(−2)	0.130(−3)	0.650(−3)	0.498(−4)	0.249(−3)	0.257(−4)	0.128(−3)
0.488(−3)	0.244(−2)	0.103(−3)	0.514(−3)	0.437(−4)	0.219(−3)	0.238(−4)	0.119(−3)
0.339(−3)	0.169(−2)	0.817(−4)	0.408(−3)	0.376(−4)	0.188(−3)	0.197(−4)	0.986(−4)
0.227(−3)	0.113(−2)	0.648(−4)	0.324(−3)	0.344(−4)	0.172(−3)	0.196(−4)	0.979(−4)
0.145(−3)	0.724(−3)	0.533(−4)	0.267(−3)	0.326(−4)	0.163(−3)	0.206(−4)	0.103(−3)
0.975(−4)	0.488(−3)	0.429(−4)	0.215(−3)	0.295(−4)	0.147(−3)	0.193(−4)	0.965(−4)
0.855(−4)	0.427(−3)	0.343(−4)	0.171(−3)	0.254(−4)	0.127(−3)	0.169(−4)	0.845(−4)
0.107(−3)	0.536(−3)	0.293(−4)	0.147(−3)	0.198(−4)	0.988(−4)	0.127(−4)	0.634(−4)
0.160(−3)	0.802(−3)	0.277(−4)	0.139(−3)	0.142(−4)	0.713(−4)	0.837(−5)	0.418(−4)
0.236(−3)	0.118(−2)	0.315(−4)	0.158(−3)	0.108(−4)	0.540(−4)	0.581(−5)	0.290(−4)
0.316(−3)	0.158(−2)	0.398(−4)	0.199(−3)	0.998(−5)	0.499(−4)	0.526(−5)	0.263(−4)
0.387(−3)	0.193(−2)	0.483(−4)	0.242(−3)	0.124(−4)	0.618(−4)	0.758(−5)	0.379(−4)
0.437(−3)	0.218(−2)	0.554(−4)	0.277(−3)	0.154(−4)	0.770(−4)	0.103(−4)	0.515(−4)
0.456(−3)	0.228(−2)	0.587(−4)	0.294(−3)	0.164(−4)	0.822(−4)	0.110(−4)	0.552(−4)

their experimental results as well as with those of other experimentalists. Here we give the FOMBT results for the six levels studied in the present work in tabulated form in Table IV and in Figs. 6–9 we compare them with the experimental results of Register *et al.*[9] and also with other theoretical results.

Figures 6(a) and 6(b) show the FOMBT and the experimental results[9] for the ICS of the $3s'[\frac{1}{2}]_1(^1P_1)$ level and of the complete manifold $3s,3s'$ compared with DWA and MCDA calculational results[28,34,35] (for the $^1P_1$ level) and DWA and VPSA calculational results[28,30] (for the complete manifold). In general, the FOMBT calculational results are in better agreement with the experiment than the other theoretical results, although the DWA results of Balashov *et al.*[35] for the $^1P_1$ level are closer to the experimental values than the FOMBT ones for energies below

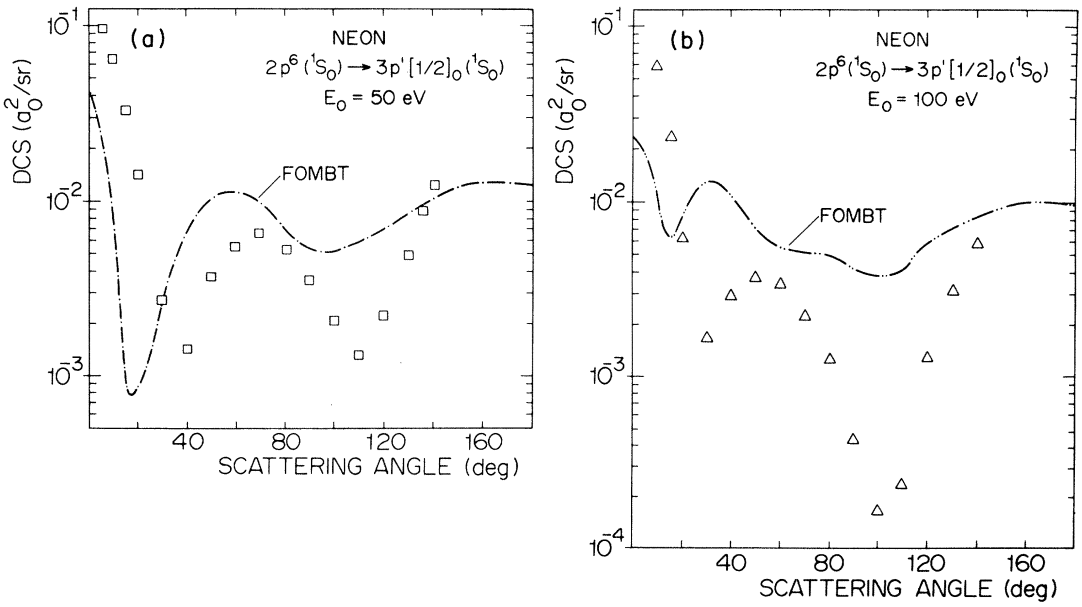

FIG. 5. DCS for the $3p'[\frac{1}{2}]_0(^1S_0)$ level of neon, with the inclusion of the spin-orbit coupling. In both graphs the curves are the FOMBT results and squares (□) and triangles (△) are the experimental points of Ref. 9. The incident electron energies are (a) 50 eV and (b) 100 eV. [Final-state wave function is given by Eqs. (7a) and (7c).]

TABLE III. Differential cross sections (in A_0^2/sr) for electron-impact excitation of the $3p'[\frac{1}{2}]_0(^1S_0)$ and $3p[\frac{1}{2}]_0(^3P_0)$ levels of neon using the FOMBT.

Incident energy (eV) / Final level / Angle (deg)	22.13		36.0		50.0		80.0		100.0	
	$3p'[\frac{1}{2}]_0$	$3p[\frac{1}{2}]_0$	$3p'[\frac{1}{2}]_0$	$3p[\frac{1}{2}]_0$	$3p'[\frac{1}{2}]_0$	$3p[\frac{1}{2}]_0$	$3p'[\frac{1}{2}]_0$	$3p[\frac{1}{2}]_0$	$3p'[\frac{1}{2}]_0$	$3p[\frac{1}{2}]_0$
0	0.599(−2)[a]	0.120(−3)	0.198(−1)	0.396(−3)	0.438(−1)	0.876(−3)	0.208(−1)	0.416(−3)	0.237(−1)	0.474(−3)
10	0.592(−2)	0.119(−3)	0.121(−1)	0.245(−3)	0.705(−2)	0.142(−3)	0.900(−2)	0.181(−3)	0.102(−1)	0.205(−3)
20	0.580(−2)	0.117(−3)	0.670(−2)	0.138(−3)	0.883(−3)	0.210(−4)	0.337(−2)	0.704(−4)	0.860(−2)	0.174(−3)
30	0.570(−2)	0.116(−3)	0.644(−2)	0.134(−3)	0.290(−2)	0.620(−4)	0.893(−2)	0.181(−3)	0.134(−1)	0.269(−3)
40	0.566(−2)	0.116(−3)	0.810(−2)	0.167(−3)	0.710(−2)	0.145(−3)	0.102(−1)	0.206(−3)	0.107(−1)	0.214(−3)
50	0.551(−2)	0.115(−3)	0.977(−2)	0.201(−3)	0.105(−1)	0.213(−3)	0.856(−2)	0.179(−3)	0.711(−2)	0.143(−3)
60	0.535(−2)	0.115(−3)	0.990(−2)	0.206(−3)	0.116(−1)	0.234(−3)	0.706(−2)	0.143(−3)	0.566(−2)	0.114(−3)
70	0.513(−2)	0.114(−3)	0.902(−2)	0.192(−3)	0.990(−2)	0.200(−3)	0.626(−2)	0.126(−3)	0.531(−2)	0.106(−3)
80	0.489(−2)	0.112(−3)	0.756(−2)	0.165(−3)	0.687(−2)	0.140(−3)	0.550(−2)	0.110(−3)	0.499(−2)	0.100(−3)
90	0.451(−2)	0.107(−3)	0.607(−2)	0.135(−3)	0.530(−2)	0.110(−3)	0.456(−2)	0.923(−4)	0.433(−2)	0.875(−4)
100	0.420(−2)	0.103(−3)	0.512(−2)	0.115(−3)	0.527(−2)	0.108(−3)	0.393(−2)	0.811(−4)	0.393(−2)	0.803(−4)
110	0.396(−2)	0.975(−4)	0.529(−2)	0.117(−3)	0.588(−2)	0.113(−3)	0.469(−2)	0.973(−4)	0.438(−2)	0.899(−4)
120	0.382(−2)	0.929(−4)	0.669−2)	0.143(−3)	0.688(−2)	0.143(−3)	0.723(−2)	0.146(−3)	0.600(−2)	0.123(−3)
130	0.379(−2)	0.894(−4)	0.781(−2)	0.163(−3)	0.856(−2)	0.176(−3)	0.980(−2)	0.200(−3)	0.736(−2)	0.151(−3)
140	0.386(−2)	0.872(−4)	0.874(−2)	0.179(−3)	0.105(−1)	0.213(−3)	0.119(−1)	0.240(−3)	0.860(−2)	0.175(−3)
150	0.396(−2)	0.854(−4)	0.943(−2)	0.191(−3)	0.120(−1)	0.242(−3)	0.130(−1)	0.263(−3)	0.961(−2)	0.195(−3)
160	0.404(−2)	0.837(−4)	0.978(−2)	0.197(−3)	0.127(−1)	0.256(−3)	0.138(−1)	0.278(−3)	0.103(−1)	0.207(−3)
170	0.413(−2)	0.835(−4)	0.101(−1)	0.202(−3)	0.128(−1)	0.257(−3)	0.142(−1)	0.284(−3)	0.104(−1)	0.208(−3)
180	0.417(−2)	0.833(−4)	0.973(−2)	0.195(−3)	0.124(−1)	0.248(−3)	0.138(−1)	0.276(−3)	0.990(−2)	0.198(−3)

[a]The notation 0.599(−2) means 0.599×10^{-2}.

TABLE IV. Integral cross sections (in 10^{-20} cm^2) for the $3s'[\frac{1}{2}]^o_1$, $3s[1\frac{1}{2}]^o_1$, $3s'[\frac{1}{2}]^o_0$, $3s[1\frac{1}{2}]^o_2$, $3p'[\frac{1}{2}]_0$, and $3p[\frac{1}{2}]_0$ levels of neon using the FOMBT.

Energy (eV) \ Final level	$3s'[\frac{1}{2}]^o_1$	$3s[1\frac{1}{2}]^o_1$	$3s'[\frac{1}{2}]^o_0$	$3s[1\frac{1}{2}]^o_2$	$3p'[\frac{1}{2}]_0$	$3p[\frac{1}{2}]_0$
20.0	144.0	97.3	30.5	152.5		
22.13					164.0	3.66
30.0	589.3	133.5	30.9	154.6		
36.0					272.0	5.74
40.0			20.3	101.6		
50.0	919.0	107.1	12.6	62.3	277.0	5.60
80.0			3.2	16.1	265.0	5.40
100.0	884.9	72.6	1.57	7.9	239.0	4.80
120.0			0.89	4.5		

50 eV.

In Fig. 6(b) the results of a VPSA calculation reported by Theodosiou[30] disagree strongly with all the other results, and the experimental data are restricted to energies of 50 eV or less but the FOMBT results show a broad maximum at around 70 eV which should be confirmed by experiment.

In Fig. 7 we show the results for the ICS of the "^3P level", namely, for the sum of cross sections of the $3s[\frac{1}{2}]^o_0$, $3s[1\frac{1}{2}]^o_1$, and $3s'[1\frac{1}{2}]^o_2$ triplet levels. The DWA calculation of Sawada *et al.*[34] does not show, in this case the peak in the ICS around $C=30$ eV, that is observed in the experiment and obtained also in the FOMBT. The FOMBT shows correctly the position of this peak but disagrees at that point by about 30% with the experimental value obtained by Register *et al.*[9] There are no experimental results for energies above 50 eV, but an extrapolation of the data reported by Register *et al.*[9] to higher energies indicates good agreement with the FOMBT results.

For levels of the $2p^5 3p$ final state configuration of Ne the overall agreement becomes worse as shown in Fig. 8 for the $3p'[\frac{1}{2}]_0(^1S_0)$ level. Both the FOMBT calculation and Born and Born-Ochkur approximation calculation of Sharpton *et al.*[17] disagree in shape with the experimental results of Register *et al.*[9] The results of another Born-Ochkur approximation calculation, by Lins de Barros and Brandi[33] yielded cross sections which are by about a factor of 10 lower than the experimental results. (The corresponding results of Boikova and Fradkin[26] were not reproduced here because it was too difficult to extract them

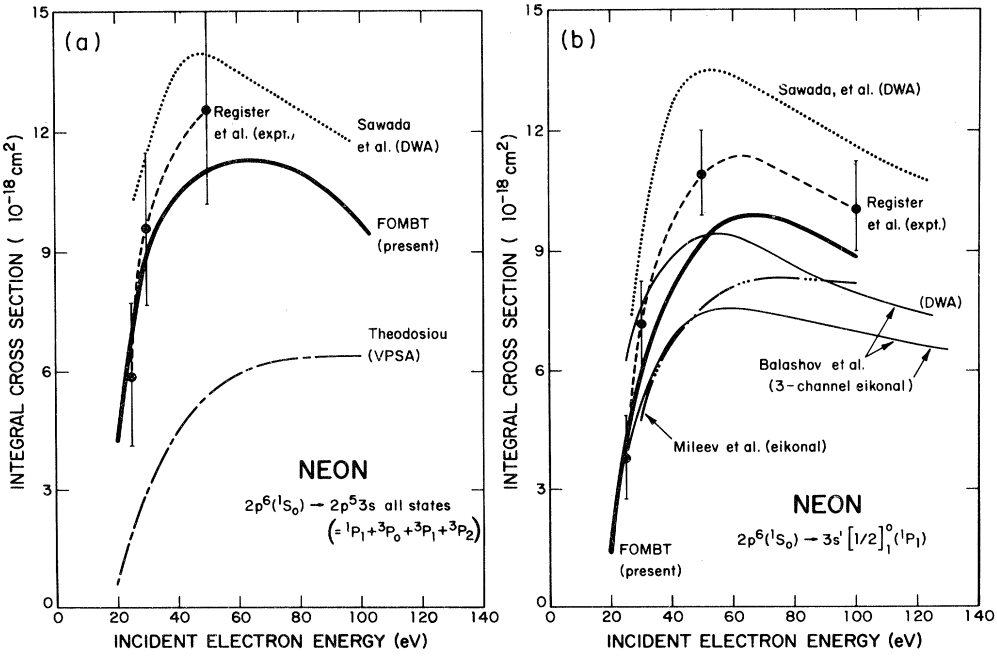

FIG. 6. (a) Integral cross sections (ICS) for the excitation of the $3s[\frac{1}{2}]^o_1(^1P_1)$ level of neon. The heavy solid curve denotes the result of FOMBT and the points with error bars are the experimental points of Ref. 9. Other theoretical results are as indicated. [Final-state wave function is given by Eqs. (7b) and (7c).] (b) Same for (a), except for the total $3s,3s'$ manifold.

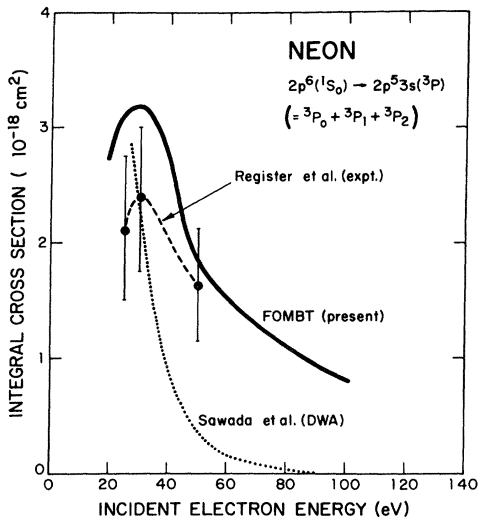

FIG. 7. Same as for Fig. 6, except for the $^3P(3s[1\frac{1}{2}]_1^o + 3s[\frac{1}{2}]_0^o + 3s'[1\frac{1}{2}]_2^o)$ level of neon.

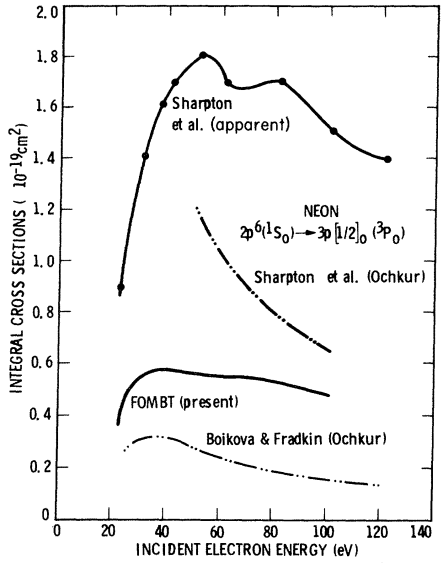

FIG. 9. ICS for the excitation of the $3p[\frac{1}{2}]_0(^3P_0)$ level of neon. The heavy solid curve is the result of FOMBT and the light solid curve is the experimental result of Sharpton *et al.* (Ref. 17). The dashed curves are other theoretical results, as indicated.

from the published figures with reliability.) Their ICS results are comparable to the experimental results of Register *et al.*[9] In Fig. 9 we show the results for the $3p[\frac{1}{2}]_0(^3P_0)$ level. Since this level was not resolved in the experiment of Register *et al.*,[9] we compare the FOMBT results with the experimental apparent excitation cross section results of Sharpton *et al.*[17] as well as with the Born-Ochkur results of Sharpton *et al.*[17] and of Boikova and Fradkin.[26] These last results were reproduced from a graph given by Lins de Barros and Brandi[33] after correcting for a scale error that occured in their work. The various results again disagree with each other both in absolute value and in shape. In this case, Lins de Barros and Brandi results are about a factor of three higher than the experimental results. The FOMBT result exhibits a very broad maximum not shown by any of the previous results. Here we have to remember that, as pointed by Sharpton *et al.*[17] the corrections due to cascade contributions (not included in any theoretical calculation) can play a decisive role. Obviously all of the facts listed in the end of the previous section in connection with difficulties in our calculations for $3p, 3p'$ levels remains valid for the calculation of the ICS's.

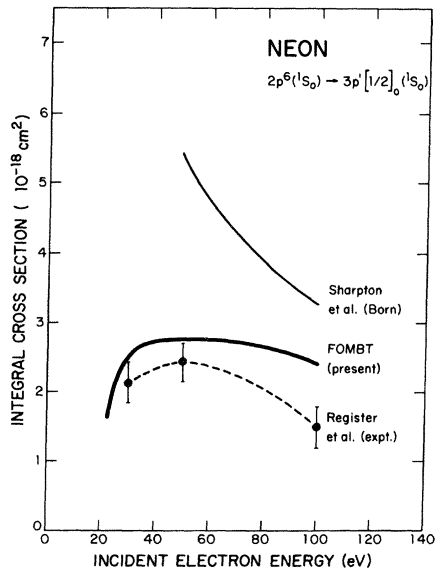

FIG. 8. Same as for Fig. 6, except for the $3p'[\frac{1}{2}]_0(^1S_0)$ level of neon.

C. Conclusions and summary

The results of this study show that the FOMBT, with incorporation of spin-orbit coupling effects in the target states, gives the best results for excitation of the $^1P_1$ optically allowed levels among the levels studied here. Identical conclusion was obtained by Padial *et al.*[55] in the case of argon and Thomas *et al.*[53] for He. The theoretical results for the $^1P_1$ level agree within about 15% with experiment in the $10° \leq \theta \leq 80°$ angular range and the agreement improves with increasing energy. For an incident electron energy of $E = 100$ eV, the same agreement is found for the entire experimentally studied angular range: $10° \leq \theta \leq 140°$. The good results obtained for the excitation of the $^1P_1$ level can be rationalized in the following way: This is an optically allowed (resonance) transition and the electron-impact process is dominated by the single $S \rightarrow P$ direct excitation controlled by the dipole transition potential which is correctly taken into account in the FOMBT. The influence of second-order processes and higher-order exchange terms on the DCS in the $10° < \theta < 80°$ angular range appear to be small. For $\theta < 10°$ angles, polarization effects (second-order processes) might prove to be important and for $\theta > 80°$ angles higher-order exchange effects could play a significant role.

The present results also show the importance of incor-

porating target spin-orbit coupling effects for calculation of the electron-impact excitation of the $^3P_1$ level of neon. If spin-orbit coupling is included into the wave functions of the $^3P_1$ level the FOMBT DCS gives an agreement better than 10% with experiment for the $10° \leq \theta \leq 80°$ angular range while results from a pure *LS*-coupled model are in substantial disagreement with experiment in the same angular range. Again the agreement between FOMBT and experimental results improve with increasing energy.

The FOMBT results for the excitation of $^3P_0$ and $^3P_2$ metastable levels are in less satisfactory agreement with experiment. There is reasonable agreement between FOMBT and experimental DCS (the discrepancies are around 10% larger than the experimental errors) for these levels in the $30° \leq \theta \leq 90°$ angular range and qualitative similarity with respect to the shapes of the DCS's but the results clearly show that the effects (channel-coupling, back-coupling, and final-state effects) absent in the FOMBT are important for the accurate calculation of the electron-impact excitation of these levels. Of the excitation processes studied in this work, the FOMBT has the most difficulty in treating the excitation of the $^1S_0$ level. In particular, the agreement between the FOMBT and the experimental results for the DCS for the excitation of that level becomes poorer as the energy increases for reasons that are not obvious at this time.

In general, the same conclusions can be drawn for the ICS results. The FOMBT gives the best results for the excitation of the $^1P_1$ level and the discrepancies between FOMBT results and the experimental results of Register *et al.*[9] for the excitation of the ^3P level (Fig. 7) are at some energies, slightly larger than the experimental errors. These discrepancies become even larger when one considers the ICS for the excitation of level $3p'[\frac{1}{2}]_0(^1S_0)$ and $3p[\frac{1}{2}]_0(^3P_0)$. Particularly for this last level the strong disagreement among available experimental and calculational results makes difficult to draw any general conclusion. It is noteworthy, however, that even for these transitions the FOMBT gives better results for the ICS than the results obtained from previous Born calculations.

ACKNOWLEDGMENTS

The authors gratefully acknowledge the joint support of the U.S.—Latin American Cooperative Science Program, National Science Foundation (O.I.P), and Conselho Nacional de Desenvolvimento Científico e Tecnólogico (Brazil) which made this research possible. One of us (L.E.M.) acknowledges the financial support of the Fundacão de Amparo a Pesquisa do Estado de São Paulo (Brazil). We also express our gratitude to Dr. David C. Cartwright of Los Alamos National Laboratory and Dr. Sandor Trajmar of the Jet Propulsion Laboratory for fruitful discussions and valuable help, and to Dr. Robert D. Cowan of Los Alamos National Laboratory for providing the spin-orbit coupling wave functions used in our calculations. The authors also thank Professor Vincent McKoy for critically reading the manuscript.

---

*Permanent address: Departamento de Fisica, Universidade Federal de São Carlos, 13560 São Carlos, São Paulo, Brazil.

†Present and permanent address.

[1]See, e.g., L. A. Levin, S. E. Moody, E. L. Klosterman, R. E. Center, and J. J. Ewing, IEEE J. Quantum Electron QE-17, 2282 (1981).

[2]E. U. Condon and G. H. Shortley, *The Theory of Atomic Spectra* (Cambridge University Press, New York, 1935), pp. 201—315.

[3]See, e.g., B. H. Bransden and M. R. C. McDowell, Phys. Rep. 46, 249 (1978) for a review. The spectroscopic notation of this work is adopted here. Occasionally the closest approximation *LS*-coupled state will be given in parenthesis.

[4]S. K. Srivastava, H. Tanaka, A. Chutjian and S. Trajmar, Phys. Rev. A 23, 2156 (1981).

[5]A. Chutjian and D. C. Cartwright, Phys. Rev. A 23, 2178 (1981).

[6]S. Trajmar, S. K. Srivastava, H. Tanaka, H. Nishimura, and D. C. Cartwright, Phys. Rev. A 23, 2167 (1981).

[7]$4s,4s'$ levels will refer to the collection of levels $4s[1\frac{1}{2}]^o_1$, $4s[1\frac{1}{2}]^o_2$, $4s'[\frac{1}{2}]^o_2$ and $4s'[\frac{1}{2}]^o_1$ of argon using the notation of Ref. 3. $3s,3s'$ levels have identical meaning for the corresponding levels of neon.

[8]D. F. Register and S. Trajmar, this issue, Phys. Rev. A 29, 1785 (1984).

[9]D. F. Register, S. Trajmar, G. Steffensen, and D. C. Cartwright, preceding paper, Phys. Rev. A 29, 1793 (1984).

[10]W. C. Tam and C. E. Brion, J. Electron Spectrosc. Rel. Phen. 2, 11 (1973).

[11]The notation of Ref. 3 is used here.

[12]D. Roy and J.-D. Carette, Can. J. Phys. 52, 1178 (1974).

[13]F. H. Nicoll and C. B. O. Mohr, Proc. Roy. Soc. (London) A 142, 647 (1933).

[14]W. Hanle, Z. Phys. 65, 512 (1930).

[15]O. Herrmann, Ann. Phys. 25, 143 (1936).

[16]I. P. Zapesochnyi and P. V. Feltsan, Bull. Acad. Sci. USSR Phys. Ser. 27, 1015 (1963).

[17]F. A. Sharpton, R. M. St. John, C. C. Lin, and F. E. Fajen, Phys. Rev. A 2, 1305 (1970).

[18]J. P. de Jongh, Thesis, University of Utrecht (1971) (unpublished).

[19]A. F. J. van Raan, Physica (Utrecht) 65, 566 (1973).

[20]K.-H. Tan, F. G. Donaldson, and J. W. McConkey, Can. J. Phys. 52, 788 (1974).

[21]M. H. Phillips, L. W. Anderson, and C. C. Lin, Phys. Rev. A 23, 2751 (1981).

[22]R. E. Miers, J. E. Gastineau, M. H. Phillips, L. W. Anderson, and C. C. Lin, Phys. Rev. A 25, 1185 (1982).

[23]P. J. O. Teubner, J. L. Riley, M. C. Tonkin, J. E. Furst, and S. J. Buckman, in *Abstracts of Contributed Papers, XII International Conference on the Physics of Electronic and Atomic Collisions,* edited by S. Datz, (ICPEAC, Gatlinburg, 1981), p. 153.

[24]H. S. W. Massey and C. B. O. Mohr, Proc. Roy. Soc. A 146, 880 (1934).

[25]V. Ya. Veldre, A. V. Lyash, and L. L. Rabik, Opt. Spektrosk. 19, 319 (1965) [Opt. Spectrosc. USSR 19, 182 (1965)].

[26]R. F. Boikova and E. E. Fradkin, Opt. Spektrosk. 19, 843 (1965) [Opt. Spectrosc. USSR 19, 470 (1965)].
[27]R. Albat and N. Gruen, J. Phys. B 7, L9 (1974).
[28]V. N. Mileev, V. I. Safin, and S. I. Strakhova, J. Phys. B 11, 2941 (1978).
[29]V. V. Karapetjan, V. N. Mileev, and N. N. Titarenko, Nucl. Phys. A 203, 561 (1973).
[30]C. E. Theodosiou, J. Phys. B 13, L113 (1980).
[31]L. Vainshtein, L. Presnyakov and I. Sobel'man, Zh. Eksp. Teor. Fiz. 45, 2015 (1963). [Sov. Phys.—JETP 18, 1383 (1964)].
[32]P. S. Ganas and A. E. S. Green, Phys. Rev. A 4, 182 (1971).
[33]H. G. P. Lins de Barros and H. S. Brandi, Can. J. Phys. 53, 689 (1975).
[34]T. Sawada, J. E. Purcell, and A. E. S. Green, Phys. Rev. A 4, 193 (1971).
[35]V. V. Balashov, I. V. Kozhevnikov, and A. I. Magunov, J. Phys. B 14, 2059 (1981).
[36]H. Feshbach and J. Hüfner, Ann. Phys. N. Y. 56, 268 (1970).
[37]Gy. Csanak, H. S. Taylor, and R. Yaris, Phys. Rev. A 3, 1322 (1971); Adv. At. Mol. Phys. 7, 287 (1971).
[38]T. N. Rescigno, C. W. McCurdy, and V. McKoy, J. Phys. B 7, 2396 (1974).
[39]M. S. Pindzola and H. P. Kelly, Phys. Rev. A 11, 221 (1975).
[40]R. V. Calhoun, D. H. Madison, and W. N. Shelton, Phys. Rev. A 14, 1380 (1976).
[41]D. H. Madison, J. Phys. B 12, 3399 (1979).
[42]K. H. Winters, J. Phys. B 11, 149 (1978).
[43]B. H. Bransden and M. R. C. McDowell, Phys. Rep. 30C, 207 (1977).
[44]N. F. Mott and H. S. W. Massey, *The Theory and Atomic Collisions,* 3rd ed. (Clarendon Press, Oxford, 1965) pp. 349—351.
[45]H. A. Bethe and R. Jackiw, *Intermediate Quantum Mechanics* (Benjamin, New York, 1968) pp. 294—320.
[46]H. S. W. Massey, E. H. S. Burhop, and H. B. Gilbody, *Electronic and Ionic Impact Phenomena* (Oxford University Press, Oxford, 1969), Vol. 1 Chap. 8.
[47]I. I. Sobel'man, L. A. Vainhstein, and E. A. Yukov, *Excitations of Atoms and Broadening of Spectral Lines* (Springer, Berlin, 1981), pp. 46—64.
[48]B. L. Moiseiwitsch and S. J. Smith, Rev. Mod. Phys. 40, 238 (1968).
[49]Gy. Csanak, H. S. Taylor, and D. N. Tripathy, J. Phys. B 6, 2040 (1973).
[50]P. G. Burke and H. M. Schey, Phys. Rev. 126, 147 (1962).
[51]P. G. Burke, A. Hibbert, and W. D. Robb, J. Phys. B 4, 153 (1972).
[52]W. C. Fon, P. G. Burke, K. A. Berrington, and A. H. Hibbert, J. Phys. B 16, 307 (1983).
[53]L. D. Thomas, Gy. Csanak, H. S. Taylor, and B. S. Yarlagadda, J. Phys. B 7, 1719 (1974).
[54]A. Chutjian and L. D. Thomas, Phys. Rev. A 11, 1583 (1975).
[55]N. T. Padial, G. D. Meneses, F. J. da Paixão, Gy. Csanak, and D. C. Cartwright, Phys. Rev. A 23, 2194 (1981).
[56]L. E. Machado, E. P. Leal, and Gy. Csanak, J. Phys. B 15, 1773 (1982).
[57]The random phase approximation for the transition density matrix has been discussed for atomic and molecular systems by (a) P. L. Altick and A. E. Glassgold, Phys. Rev. 133, 632 (1964); (b) T. H. Dunning and B. V. McKoy, J. Chem. Phys. 47, 1735 (1967); (c) A. D. McLachlan and M. A. Ball, Rev. Mod. Phys. 36, 844 (1964).
[58]K. Schackert, Z. Phys. 213, 316 (1968).
[59]The FCHF approximation is discussed in detail by G. Bates, [Comp. Phys. Commun. 8, 220 (1974)] along with its numerical solution.
[60]R. D. Cowan and K. L. Andrew, J. Opt. Soc. Am. 55, 502 (1965).
[61]R. D. Cowan, J. Opt. Soc. Am. 58, 808 (1968), 58, 924 (1968).
[62]R. D. Cowan, private communication.
[63]The Hartree-Fock equations for the $[(2)^5 3s]^1P_1$ and $[(2p)^5 3s]^3P_1$ states of neon are discussed by A. Gold and R. S. Knox [Phys. Rev. 113, 834 (1959)]. In the present work the equations in the first column on p. 835 were solved for the $3s$ orbital using the ground-state orbitals for $1s$, $2s$, and $2p$ (FCHF approximation).
[64]D. C. Cartwright, A. Chutjian, S. Trajmar, and W. Williams, Phys. Rev. A 16, 1013 (1977).